Photoionization rate in wide band-gap crystals

V. E. Gruzdev
Department of Mechanical and Aerospace Engineering, University of Missouri-Columbia, Columbia, Missouri 65211, USA
(Received 27 March 2006; revised manuscript received 25 August 2006; published 11 May 2007)

The Keldysh model of the photoionization [L. V. Keldysh, Sov. Phys. JETP **20**, 1307 (1965)] is extended by deriving a formula for the photoionization rate of crystals based on the cosine energy-momentum relation. The relation is characteristic of tight-binding approximation and directly takes into account the influence of Bragg-type reflections of oscillating electrons at the edges of the first Brillouin zone. Due to the reflections and oscillations, the dependence of the photoionization rate on laser and material parameters takes form of a multibranch function with the branches separated by singularity points with unlimited increasing of the rate. Each of the singularities is coupled to the flattening of the effective-band structure. The laser intensity corresponding to the first singularity is found to be about 10 TW/cm^2 for most wide band-gap crystals. We also show that the lowest-order branch of the photoionization rate completely corresponds to the multiphoton regime, and the first singularity takes place before the tunneling regime starts to dominate. Analysis of the ionization-rate asymptotic in the vicinity of the first-singularity point suggests possibility of ionization suppression by high-intensity radiation for certain ranges of laser wavelength.

DOI: 10.1103/PhysRevB.75.205106 PACS number(s): 78.47.+p, 42.50.Ct, 42.50.Hz, 81.40.Tv

I. INTRODUCTION

Due to the importance of understanding laser-pulse propagation and most laser-solid interactions, theoretical study of laser-induced photoionization of crystalline solids transparent at input laser wavelength has attracted great attention since the early days of laser epoch.[1,2] Recently, more attention has been paid to the problem of photoionization with photon energy $\hbar\omega$ much smaller than material band gap due to active investigations of femtosecond laser interactions with wide band-gap materials.[3–12] Small duration of the ultrashort pulses provides specific conditions for the interactions. For example, intensity of a femtosecond pulse propagating in the wide band-gap solids without damaging them can reach 10 TW/cm^2 or even exceed that level.[3–12] Moreover, it has been shown[13] that the photoionization becomes a dominating ionization mechanism in nonmetallic solids at that high-intensity level if pulse duration is shorter than 1 ps. Those facts make actual the problem of proper description of the photoionization of wide band-gap solids by laser radiation.

The pioneering models of the photoionization were based on the standard procedure of the classical perturbation theory.[1,2,14–18] They served as a starting point to develop understanding of the photoionization regularities, in particular, the influence of energy-band structure of crystals on the value of the photoionization rate.[2,18] However, specific procedure of the traditional perturbation approach did not allow calculating the probability of the multiphoton ionization of the order higher than 4 and that put strong limitations on the range of laser parameters for which those models were valid. In particular, that problem blocked transferring the perturbation-theory results to the domain of intensity exceeding 1 TW/cm^2 for most transparent solids.[2]

In 1964, Keldysh proposed a new approach[19] to solve the problem of theoretical description of the photoionization. It had several important advantages over other models. First, Keldysh overcame the calculation problems of the traditional perturbation theory and derived formulas describing ionization rate for arbitrary number of absorbed photons. As compared to the traditional perturbation approaches,[1,2,14–18] the Keldysh model significantly increased the range of laser and material parameters in which the photoionization rate can be calculated. Second, Keldysh showed the possibility of one more regime of the photoionization referred to as high-frequency tunneling that dominates at high laser intensity. Third, he showed that multiphoton and tunneling regimes are only the two limiting cases of a general ionization process. The former corresponds to low intensity and high frequency, while the latter corresponds to high intensity and relatively low frequency of radiation. Transition between the two regimes is regulated by the Keldysh adiabatic parameter,[19]

$$\gamma = \frac{\omega\sqrt{m\Delta}}{eF}, \tag{1}$$

where ω is the laser frequency, Δ is the band gap, m is the reduced effective electron-hole mass, F is the strength of electric field of the laser radiation, and e is the electron charge. One of the greatest advantages of the Keldysh approach is that it provides possibility of clear and fast qualitative analysis of the photoionization mechanism by evaluating the adiabatic parameter [Eq. (1)].

Actually, Keldysh proposed a very specific formulation of the perturbation theory,[19] resulting in strong exponential dependence of the ionization rate on electric field of the laser radiation. His approach is very general and can be applied to describe the photoionization of different objects from single atoms to crystals. Due to that generality, the Keldysh model has attracted much attention[20–36] and has become one of the standard tools in the theory of laser photoionization. Accordingly, we employ the Keldysh approach as a basis for our calculations presented in this paper. To explain the role of our calculation in the overall scheme of that field, we give a brief review of the challenges researchers have met improving the Keldysh model.

The main problem of the Keldysh approach is a number of obvious and nonobvious limitations[20,21] related to the mathematical methods employed in his calculations, e.g., the saddle-point asymptotical integration and the assumption on small initial value of the electron kinetic momentum. The assumptions and the unusual formulation of the perturbation theory given by Keldysh resulted in intensive criticism of his approach[16,22–25,30] accompanied by improvements and reformulations of the Keldysh theory. The first improvement came from applying the velocity-gauge formalism and the *S*-matrix formalism[22,26–28] that allowed removing some of the initial limitations of the Keldysh approach and showed its relation to the traditional perturbation-theory results at low intensity.[26,29] Also, relation of the Keldysh approach to more general strong-field approximations was established[28,30] by utilizing various gauges. Later attempts were done to include some higher-order corrections into the Keldysh formula for the photoionization of atoms and to find an appropriate gauge, making the overall formulation of the Keldysh approach straightforward and unambigious.[30–32] Finally, it was shown[33] that the length gauge matches exactly the numerical solution of the time-dependent Schrodinger equation and is more natural than the velocity gauge.

Other important challenges met by the researchers were related to the approximation of small initial value of kinetic momentum of the electrons excited by the laser radiation. In the case of atom ionization, that assumption is of principal importance[34] since it significantly limits the kinetic energy of photoelectrons. In the case of laser ionization of nonmetallic crystals, that approximation looks quite natural[20] and shows that the main contribution to interband transitions is made by the electrons occupying initial states near the minimum point of the forbidden-energy band. Recently,[34,36] a significant improvement was done in that direction, and the assumption was removed completely in some particular cases (e.g., electron detachment from negative ions[34]), but in general case (electron detachment from neutral atom or a positive ion) it still stays a challenge.

The problem of the limitation put by the saddle-point method has also been attacked[35,36] to remove the limitation that affected the description of the photoionization in the tunneling regime. It was shown[35,36] that a rigorous integration is possible under the assumption of small values of the adiabatic parameter [Eq. (1)], and the limitation was completely removed in that particular regime, but it is still a challenge for the regime of low-intensity multiphoton ionization.[24,27,30]

Most of those modifications of the Keldysh approach[22,25–37] are related to developing the formal procedure of the Keldysh model and improving its mathematical methods. On the other hand, the modifications were done only for two specific energy-momentum relations—the parabolic one[22,26–37] or the Kane-type[25,37] one. The parabolic relation is very natural for the case of laser ionization of atoms if the energy of the photoelectrons is small enough to apply the nonrelativistic approximation. In the case of the nonmetal crystals, the parabolic relation describes only small vicinity of a minimum point of the forbidden band. The latter is also true for the Kane-type dispersion relation[38] that is more specific for narrow-gap semiconductors.

Utilizing those particular energy-momentum relations puts an additional limitation on the range of laser intensity for which the Keldysh formula and its modifications are valid. For example,[20,39] in the particular case of the nonmetallic crystals, the value of laser intensity must not exceed several $\mathrm{TW/cm}^2$ for the photoionization to be reliably described on the basis of the parabolic or the Kane-type relations. It means that both the Keldysh formula in its traditional formulation[19] and its modified versions[22–37] do not provide reliable value of the photoionization rate of transparent solids at intensity exceeding that limit. To extend the Keldysh model to the range of higher intensities, one should utilize a more general energy-momentum relation rather than the parabolic and the Kane-type ones. Moreover, recent analysis of the physical aspects of the Keldysh model has shown[20,21,39] that in general case his formula for the ionization rate must significantly depend on the energy-momentum relation that determines the exponential factor in the formula.[19]

One more aspect of this problem is of key importance for the theoretical description of the ionization processes. On the one hand, Keldysh[19] showed a great degree of similarity between photoionization of single atoms and solids. On the other hand, a significant difference between the crystals and single atoms is that the dynamics of crystal electrons is determined by both the action of laser radiation and the action of the periodic crystal potential. The latter is described by the effective electron mass[40] that depends on the electron state in the crystal,[40] i.e., electron quasimomentum. The parabolic energy-momentum relation corresponding to constant value of the effective mass[40] can give wrong results in the case of the crystals because of the neglected influence of momentum-dependent contributions to the mass. Thus, the calculation presented below should also be considered as an attempt to take into account an exact dependence of the effective electron mass on electron quasimomentum and to determine the range of parameters for which the approximation of the constant effective mass is reasonable in the case of nonmetallic crystals.

Making an attempt to fix those problems and to study the dependence of the photoionization rate of the Keldysh model on energy-momentum relation, recently, we performed calculations of the photoionization rate for cosine relation characteristic of wide band-gap crystals.[41] This paper is a significant extension and generalization of the previous results.[41] Those improvements led to several original qualitative conclusions important for the general understanding of laser-solid interactions. Correspondingly, this paper is organized as follows. In Sec. II, we describe calculations of the ionization rate starting from discussion of the energy-momentum relations in Sec. II A. In Sec. II B, we derive the formula for the photoionization rate and study its characteristic properties. The obtained results are discussed in Sec. III including the analysis of singularity points, discussion of model limitations, comparison with experimental data, and asymptotical analysis. Conclusions are drawn in Sec. IV.

II. CALCULATIONS OF THE IONIZATION RATE

The term "band structure" is often referred to in this paper. It denotes a structure of forbidden band as a function of

electron quasimomentum $\vec{p}$ and is essentially an energy-momentum relation for an electron-hole pair in a crystal. In the simplest case of the two-band model, it is the sum of energy $\varepsilon_C(\vec{p})$ of an electron in the conduction band and the energy $-\varepsilon_V(\vec{p})$ of the corresponding hole in the valence band,

$$\varepsilon(\vec{p}) = \varepsilon_C(\vec{p}) - \varepsilon_V(\vec{p}). \tag{2}$$

For example, the following is the widely utilized parabolic band structure:

$$\varepsilon_P(\vec{p}) = \Delta\left(1 + \frac{p^2}{2m\Delta}\right), \tag{3}$$

where $p=|\vec{p}|$. Equation (3) describes a small vicinity of the minimum point of the forbidden band in general case of direct isotropic bands.

A. Cosine-band-structure model

To make the interpretation of the presented results more transparent, we consider electron transitions between two bands only—one valence band and one conduction band—and assume that the material is an ideal direct-gap crystal, i.e., the only minimum point of the band structure lies in the center of the first Brillouin zone at $\vec{p}=0$. The energy-momentum relation to be considered in this paper reads as follows:

$$\varepsilon_{COS}(\vec{p}) = \Delta\left[1 + \frac{\hbar^2}{m\Delta d_x^2} - \frac{\hbar^2}{m\Delta d_x^2}\cos\left(\frac{d_x}{\hbar}p_x\right) \times \cos\left(\frac{d_y}{\hbar}p_y\right)\cos\left(\frac{d_z}{\hbar}p_z\right)\right], \tag{4}$$

where m is the reduced effective electron-hole mass and Δ is the band gap. Here d_x, d_y, and d_z are the lattice constants and p_x, p_y, and p_z are quasimomentum components along the principle axes of the crystal lattice. A crystal with a cubic unit cell and isotropic bands is considered by letting $d_x=d_y=d_z=d$ and $m_x=m_y=m_z=m$. We also neglect possible degeneracy of the bands. Those simplifications are of no significance for the results presented below since the latter can be easily generalized for other types of crystal symmetry as it has been demonstrated earlier.[42]

The cosine energy-momentum relation [Eq. (4)] is constructed so as to meet the following requirements that are general for all crystals[40,43]:

(1) It is periodic in quasimomentum space with period $2\pi\hbar/d$.

(2) It is smooth at the edges of the first Brillouin zone along the principle crystal axes and meets the following condition there:

$$\vec{\nabla}_p \varepsilon_{COS}(\vec{p}) = 0. \tag{5}$$

Correspondingly, expression (4) determines the band structure over the entire Brillouin zone and allows correct treatment of the Bragg-type electron reflections at its edges. Also, model relation (4) is close to the band structure of alkali halide crystals,[44,45] having almost flat valence band and cosine-shaped conduction band. This is not an occasion since the alkali halides belong to the class of wide band-gap solids, which energy bands are well described by the approximation of tight binding with dominating influence of nearest-neighbor atoms. Relation (4) is characteristic of that approximation. This allows putting formula (4) into basis of a model describing the photoionization in typical wide band-gap dielectric crystals.

For small values of quasimomentum $\vec{p}$ in the vicinity of the minimum point, the band structure [Eq. (4)] reduces to parabolic relation (3). The difference between them is that the model [Eq. (4)] includes higher-order terms that play a significant role for the regions far from the center of the first Brillouin zone.[20,41] Those higher-order corrections describe deviations from the approximation of constant effective mass and influence the ionization rate at high laser intensity. To estimate the intensity at which the corrections are of importance, we expand relation (4) into series with respect to p, keeping all the powers up to the fourth,

$$\varepsilon_{COS}(\vec{p}) = \varepsilon_P(\vec{p}) - \frac{d^2}{24\hbar^2 m}[p^4 + 4(p_x^2p_y^2 + p_x^2p_z^2 + p_y^2p_z^2)], \tag{6}$$

with $\varepsilon_P(\vec{p})$ to be given by Eq. (3) and $p^2=p_x^2+p_y^2+p_z^2$. Then, time-dependent quasimomentum of the form[19]

$$\vec{p}(t) = \vec{p}_0 - \frac{e\vec{F}}{\omega}\sin(\omega t) \tag{7}$$

is substituted into Eq. (6), where $\vec{F}$ denotes the amplitude of electric field of the laser radiation. Assuming the radiation to be linearly polarized, one can estimate the contribution of the fourth-order terms of Eq. (6) by letting $\vec{p}_0=0$, $\sin(\omega t)=-1$, and $F_y=F_z=0$. If the term proportional to p^4 is much smaller than the term $\varepsilon_P(\vec{p})$ in Eq. (6), the ionization rate must be identical for the both band structures [Eqs. (3) and (4)]. That is true if the laser intensity is below the following upper limit:

$$I \ll I_{lim} \propto \frac{12\hbar^2\omega^2}{d^2e^2}. \tag{8}$$

Correspondingly, the Keldysh parameter γ must be above the following lower limit:

$$\gamma \gg \gamma_{lim} = \frac{d\sqrt{m\Delta}}{\sqrt{12}\hbar}. \tag{9}$$

For NaCl, for example, $d=0.5628$ nm, $m=0.6m_e$ (m_e is the free-electron mass), and $\Delta=8.97$ eV,[44,46] one gets $\gamma_{lim}=1.359$ and the corresponding intensity $I_{lim}\sim 1.85\times 10^{13}$ W/cm^2 at a laser wavelength of 800 nm. Establishing similar relations[21,39] between the parabolic band [Eq. (3)] and the Kane-type band[19]

$$\varepsilon_K(\vec{p}) = \Delta\sqrt{1 + \frac{p^2}{m\Delta}}, \tag{10}$$

one can show that they result in identical values of the photoionization rate under the following conditions:

$$I \ll I_{lim}^{K} \propto \frac{4\omega^2 m\Delta}{e^2} \quad \text{and} \quad \gamma \gg \gamma_{lim}^{K} = 0.5. \tag{11}$$

Comparison of conditions (8), (9), and (11) suggests that the difference between values of the ionization rate calculated for relations (3), (4), and (10) is insignificant if only conditions (8) and (9) are met since they include the range determined from conditions (11).

B. Photoionization rate

Below, we derive the formula for the ionization rate employing cosine-band structure [Eq. (4)] in the framework of the Keldysh approach[19] that has a clear physical background[20,21,39] and allows obtaining a closed-form relation between the rate and laser and material parameters. Correspondingly, we start with the following general expression for the ionization rate w,[19]

$$w = \frac{2\pi}{\hbar}\int_{VB} |L_{CV}(\vec{p}_0)|^2 \sum_{n=0}^{\infty} \delta[\varepsilon_{eff}(\vec{p}_0) - n\hbar\omega] \frac{d^3 p_0}{(2\pi\hbar)^3}, \tag{12}$$

where VB is the volume of the first Brillouin zone and $\delta(x)$ is the delta function. The function $L_{CV}(\vec{p}_0)$ reads as follows:

$$L_{CV}(\vec{p}_0) = \frac{1}{2\pi}\oint V_{CV}\left(\vec{p}_0 - \frac{e\vec{F}}{\omega}u\right) \times \exp\left[\frac{i}{\hbar\omega}\int_0^u \varepsilon\left(\vec{p}_0 - \frac{e\vec{F}}{\omega}v\right)\frac{dv}{\sqrt{1-v^2}}\right] du, \tag{13}$$

with $V_{CV}(x)$ being the matrix element of electron transition from the valence band to the conduction band in the dipole approximation.[19] In Eq. (12), ε_{eff} is the effective-band structure which is an averaged value of energy of an electron (and the corresponding hole) performing radiation-driven oscillations in the first Brillouin zone.[20,21,39] It is calculated as follows:[19]

$$\varepsilon_{eff}(\vec{p}_0) = \frac{1}{T}\int_0^T \varepsilon\left(\vec{p}_0 - \frac{e\vec{F}}{\omega}\sin(\omega t)\right) dt, \tag{14}$$

where $T=2\pi/\omega$ is the oscillation period of electric field of the laser radiation. Expressions (12)–(14) are valid in the dipole approximation under the following description of electron functions:[18]

$$\psi(\vec{r},t) = u_n[\vec{p}(t),\vec{r}]\exp\left[\frac{i}{\hbar}\left(\vec{p}(t)\vec{r} - \int_0^t \varepsilon_n[\vec{p}(\tau)]d\tau\right)\right]. \tag{15}$$

The subscript $n=C$ stays for the conduction band, and $n=V$ stays for the valence band. Time variations of electric field $\vec{f}(t)$ of the laser radiation are considered to have the simplest form,

$$\vec{f}(t) = \vec{F}\cos(\omega t). \tag{16}$$

We perform asymptotic integration in Eq. (13) by means of saddle-point technique, as described by Keldysh.[19] To do that, the saddle points u_s and the effective-band structure [Eq. (14)] should be determined for the cosine band [Eq. (4)]. Assuming components of the initial quasimomentum $\vec{p}_0$ to be small, we expand Eqs. (12)–(14) into series with respect to those small components. To compare our results with the Keldysh formula for crystals,[19] we omit the fast oscillating terms in the final expressions during integration, although it is not quite correct.[20] Following Keldysh,[19] we assume the electric field of linearly polarized laser radiation [Eq. (16)] to be directed along one of the principle crystal axes.

One of the specific features of the cosine model is a multiple set of the saddle points. For relation (4), they read as follows:

$$u_{sj} = \frac{x - s\pi}{\chi} \pm \frac{i}{\chi}\cosh^{-1}\left(\pm\frac{\hbar^2 + md^2\Delta}{\hbar^2\cos(y)\cos(z)}\right), \tag{17}$$

where $i^2=-1$ and $s=0, \pm1, \pm2, \ldots$. Subscript $j=1$ corresponds to the sign "+" and $j=2$ corresponds to the sign "−" before the imaginary part. The values x, y, and z are the normalized components of the initial quasimomentum p_{0x}, p_{0y}, and p_{0z},

$$x = \frac{p_{0x}d}{\hbar}, \quad y = \frac{p_{0y}d}{\hbar}, \quad z = \frac{p_{0z}d}{\hbar}. \tag{18}$$

For each value of s, there is a couple of complex conjugated saddle points. The sign of the argument of inverse hyperbolic cosine depends on the quasimomentum components: if $\cos(y)\cos(z)>0$, then the sign is + which corresponds to even values of s; otherwise, the sign is − and s is odd. To utilize the Keldysh procedure[19] correctly, it is reasonable to take $s=0$ and assume $\cos(y)\cos(z)>0$ since this case corresponds to the approximations of Keldysh's calculations. Below, we show that the ionization rate is a multibranch function, and each set of the saddle points corresponds to a certain branch of the function, while the Keldysh formula[19] corresponds to the lowest-order branch.

The effective-band structure can be calculated in general form,

$$\varepsilon_{eff}^{COS}(\vec{p}_0) = \Delta\left(1 + \frac{\hbar^2}{md^2\Delta}[1 - J_0(\chi)\cos x\cos y\cos z]\right), \tag{19}$$

where $J_0(\chi)$ is the Bessel function of the first kind of the zero order with modified adiabatic parameter χ determined by electric-field strength F, laser frequency ω, and crystal constant d,

$$\chi = \frac{eFd}{\hbar\omega}. \tag{20}$$

The effective-band structure [Eq. (19)], the saddle points [Eq. (17)], and the ionization rate (see below) all depend on laser intensity through the modified adiabatic parameter χ rather than through the Keldysh parameter γ. The difference between the two parameters is that χ increases with increas-

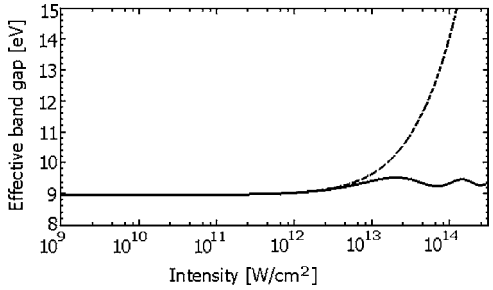

FIG. 1. Dependence of the effective band gap on laser intensity plotted for the cosine band (solid curve) and for the Kane-type band (dashed curve) calculated for parameters corresponding to NaCl and laser wavelength of 830 nm.

ing laser intensity or decreasing laser frequency, while γ decreases in both cases. Small values of the modified adiabatic parameter $\chi \ll 1$ correspond to the multiphoton regime, while the large values $\chi \gg 1$ correspond to the tunneling regime.

Recently,[21] we proposed to introduce the modified adiabatic parameter as a ratio of amplitude of radiation-driven electron oscillations to half-width of the first Brillouin zone which was based on the analysis of the physical background of the Keldysh model for laser-induced ionization of solids.[20,21,39] The expression for thus determined parameter [see Eq. 7 from Ref. 21] coincides with Eq. (20) with an accuracy of a factor of π.

For further calculations, expressions (17) and (19) are expanded into series with respect to small values of the quasimomentum components

$$x \ll 1, \quad y \ll 1, \quad \text{and} \quad z \ll 1. \tag{21}$$

Relations (21) are the standard approximation in most calculations of the ionization rate[2,14–18,22–33] except a few recent publications[34,36] which authors overcame the limitations [Eq. (21)] in certain particular cases. The limitations [Eq. (21)] are reasonable from the view point of their physical meaning: they show that the main contribution to interband transitions is given by electrons occupying the states near the minimum point of the forbidden band.[20] Neglecting all the powers of those components exceeding 2, one reduces Eq. (19) to the following relation:

$$\varepsilon_{eff}^{COS}(\vec{p}_0) = \Delta\left\{1 + \frac{\hbar^2}{md^2\Delta}[1 - J_0(\chi)] + \frac{\hbar^2}{2md^2\Delta}J_0(\chi)(x^2 + y^2 + z^2)\right\}. \tag{22}$$

A specific feature of the effective-band structures [Eq. (19) and (22)] is the oscillatory dependence of the effective band gap [obtained from Eq. (19) or (22) by letting $x=y=z=0$],

$$E = \Delta\left\{1 + \frac{\hbar^2}{md^2\Delta}[1 - J_0(\chi)]\right\}, \tag{23}$$

on laser intensity through the adiabatic parameter [Eq. (20)] (Fig. 1). In contrary to expression (23), the effective band gap of the Keldysh formula for crystals [see Eq. 38 in Ref. 21] increases monotonously with laser intensity (Fig. 1).

Contribution to the argument of the exponent of Eq. (13) from each saddle point u_{sj} calculated under conditions (21) reads as follows:

$$\begin{aligned} a_j &= \frac{i}{\hbar\omega}\int_0^{u_{sj}} \varepsilon\left(\vec{p}_0 - \frac{eF}{\omega}u\right)\frac{du}{\sqrt{1-u^2}} \\ &= -\frac{\Delta}{\hbar\omega}\left\{\frac{u_c}{u_c-1}\left[\sinh^{-1}\left(\frac{u_0}{\chi}\right) - \frac{u_0}{u_c}f_1(\chi)\right]\right. \\ &\quad \left. \mp ix\frac{u_0}{u_c-1}f_0(\chi) + \left(\frac{y^2}{2} + \frac{z^2}{2}\right)\frac{u_0}{u_c-1}f_1(\chi)\right\} \\ &\quad - \frac{\Delta}{\hbar\omega}\left[\frac{x^2}{2}\left(\frac{u_0}{u_c-1}f_1(\chi) - \sqrt{\frac{u_c+1}{(u_c-1)(\chi^2+u_0^2)}}\right)\right], \end{aligned} \tag{24}$$

where a couple of integral functions is defined by the following relations:

$$f_0(\chi) = \int_0^1 \frac{\sinh(u_0\xi)}{\sqrt{\chi^2 + u_0^2\xi^2}}d\xi, \quad f_1(\chi) = \int_0^1 \frac{\cosh(u_0\xi)}{\sqrt{\chi^2 + u_0^2\xi^2}}d\xi, \tag{25}$$

with material constants

$$u_0 = \cosh^{-1} u_c \quad \text{and} \quad u_c = 1 + \frac{md^2\Delta}{\hbar^2}. \tag{26}$$

Performing further transformations as they are described in Ref. 19, one arrives at the following expression for the ionization rate:

$$\begin{aligned} w_{COS} &= 2\frac{2\omega}{9\pi}\sqrt{\frac{\omega^3}{\hbar\Delta}}\frac{m}{dJ_0(\chi)} \\ &\quad \times \exp\left[-2\frac{u_c-1}{J_0(\chi)}\left(\left\langle\frac{E}{\hbar\omega}+1\right\rangle - \frac{E}{\hbar\omega}\right)f_2(\chi)\right] \\ &\quad \times \exp\left\{-2\frac{\Delta}{\hbar\omega}\frac{u_c}{u_c-1}\left[\sinh^{-1}\left(\frac{u_0}{\chi}\right) - \frac{u_0}{u_c}f_1(\chi)\right]\right\} \\ &\quad \times Q_{COS}\left(\chi, \frac{E}{\hbar\omega}\right), \end{aligned} \tag{27}$$

where a slow amplitude Q_{COS} is introduced in parallel to the Keldysh formula,[19]

$$Q_{COS}(\chi,s) = \sqrt{\sqrt{\frac{u_c-1}{u_c+1}(\chi^2+u_0^2)}}\sum_{n=0}^{\infty}\exp\left[-2n\frac{u_c-1}{J_0(\chi)}f_2(\chi)\right]\Phi\left[\sqrt{\frac{2(u_c-1)}{J_0(\chi)}}(\langle s+1\rangle - s + n)\sqrt{\frac{u_c+1}{(u_c-1)(\chi^2+u_0^2)}}\right]. \quad (28)$$

In Eqs. (27) and (28), the function $f_2(\chi)$ is determined through the integral $f_1(\chi)$,

$$f_2(\chi) = \frac{u_0}{u_c-1}f_1(\chi) - \sqrt{\frac{u_c+1}{(u_c-1)(\chi^2+u_0^2)}}. \quad (29)$$

The bracket $\langle x+1\rangle$ denotes the integer part of the number $x+1$, and $\Phi(x)$ is the Dawson integral,

$$\Phi(x) = \int_0^x \exp(\xi^2 - x^2)d\xi. \quad (30)$$

In contrary to the Keldysh formula, we divide the exponent of Eq. (27) into two parts. The first one includes singularities determined by the condition

$$\chi = \xi_K, \quad (31)$$

where ξ_K is the Kth root of the Bessel function $J_0(x)$. Due to specific physical meaning (see Sec. III), below we concentrate on the first singularity that occurs at $\chi=\xi_1 = 2.404\,825\,6$. Substituting this value into Eq. (20), one obtains the value of electric-field strength of laser radiation at which the first singularity occurs,

$$F_{th} = \frac{\hbar\omega}{ed}\xi_1. \quad (32)$$

This value together with the corresponding intensity is referred to as the first-singularity threshold in Sec. III.

C. Results of calculations

Figure 2 depicts the ionization rate calculated with Eq. (27) as a function of laser intensity. Calculations were performed for the parameters of NaCl (Refs. 45 and 46) and laser wavelength of 830 nm. As it was expected from the estimations [Eqs. (8) and (9)] the ionization rate [Eq. (27)] coincides with that calculated with the Keldysh formula (see Fig. 2) at low laser intensity, i.e., in the multiphoton regime. Specific feature of the ionization rate [Eq. (27)] is the set of singularities. With approaching each singularity point [Eq. (31)] from the left, the ionization rate decreases to zero and then abruptly jumps to infinity (Fig. 2).

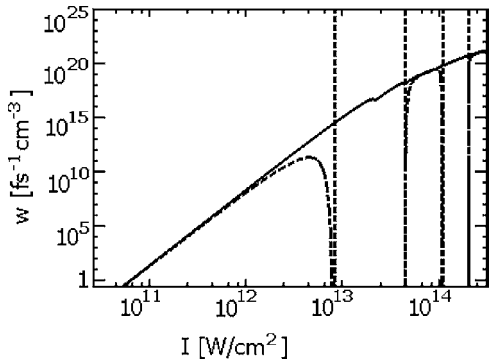

FIG. 2. Ionization rate w as a function of laser intensity I for formula (27) (dash) and the corrected Keldysh formula from Ref. 20 (solid). Material parameters correspond to NaCl; laser wavelength is 830 nm.

In the first approximation, the first-singularity threshold intensity can be evaluated from Eq. (32) under the assumption that optical parameters of the ionized area of the crystal do not vary significantly at any intensity up to the first-singularity threshold. For example, under the plane-wave approximation, the threshold of the first singularity from Fig. 2 is $I_{th}=8.3\times10^{12}$ W/cm^2.

Another remarkable feature of formula (27) is that there are certain intensity intervals for which Eq. (27) does not provide real values of the ionization rate, e.g., for $\xi_2>\chi>\xi_1$ it yields imaginary value of the rate since the argument of the Dawson function in Eq. (28) becomes negative in that case. It means that the ionization rate is a multibranch function of laser and material parameters with the branches separated by the singularities determined by the roots of the Bessel function $J_0(\chi)$. The branch of the zero order described by Eq. (27) is obtained for $0\leqslant\chi<\xi_1$ and completely corresponds to the approximations of the Keldysh formula.[19] Simple analysis of Eq. (17) shows that Eq. (27) describes also all even-order branches (Fig. 2), while study of the odd-order branches requires more complicated calculations without the assumption [Eq. (21)]. In particular, the branch next to the zero-order one is determined by the saddle points [Eq. (17)] with $s=1$ and the sign $-$ in the argument of inverse hyperbolic cosine. It corresponds to the condition $\cos y \cos z<0$ that cannot be met for small values of the components y and z of the quasimomentum. Moreover, due to the physical meaning of the first singularity discussed in the next section, it is not reasonable to analyze the high-order branches.

III. DISCUSSIONS

In this section, we discuss the physical meaning of the singularities and the mechanism of their formation. We also analyze asymptotic limits of expressions (27) and (28), the physical assumptions under which those expressions are derived and compare some predictions of the presented model with experimental data.

A. Analysis of the singularities

At first sight, the singularities in Fig. 2 seem to be unexpected and paradox since the smooth band structure [Eq. (4)]

and electron functions [Eq. (15)] are utilized to derive expressions (27) and (28). It is reasonable to associate the singularities with violation of some nonevident assumptions made in the calculation procedure or put into the basis of the Keldysh model.[20,21] To clarify that, we start with the analysis of the mathematical reasons of the singularities.

As we mentioned previously, the singularities result from the specific exponential factor of Eq. (27) that includes the Bessel function in the denominator. The presence of the Bessel function in the exponent results from the integration in the right-hand part of Eq. (13) that includes delta functions. Results of the integration are determined by the form of the effective-band structure [Eq. (22)] through the argument of the delta functions due to the following substitution:

$$\delta[\varepsilon_{eff}(\vec{p}_0) - n\hbar\omega]\frac{d^3p_0}{(2\pi\hbar)^3} = \sum_j \delta(\vec{p}_0 - \vec{p}_{0j})\left|\frac{d\varepsilon_{eff}}{d\vec{p}_0}\right|^{-1}_{p=p_{0j}}\frac{d^3p_0}{(2\pi\hbar)^3}, \quad (33)$$

made to adjust the delta-function argument and the integration variable. In Eq. (33), the vector $\vec{p}_{0j}=(x_0,y_0,z_0)\hbar/d$ is the jth root of the energy-balance equation

$$\varepsilon_{eff}(\vec{p}_0) - n\hbar\omega = 0. \quad (34)$$

Equations (22), (33), and (34) give the result,

$$\left|\frac{d\varepsilon_{eff}}{d\vec{p}_0}\right|^{-1}_{p=p_{0j}} = \frac{md}{\hbar J_0(\chi)\sqrt{x^2+y^2+z^2}}, \quad (35)$$

that makes the integral divergent if condition (31) is met. Comparing expressions (19) and (22), one can see that the Bessel function appears in the expression for the effective band and in the exponent [Eq. (27)] with no dependence on the assumptions [Eq. (21)].

The next critical point of the mathematical procedure is the saddle-point method employed to obtain the asymptotic expansion of integral (13). Performing rather extensive calculations,[47] one can see that all terms of the expansion include the same singularities with the threshold [Eq. (31)] due to relations (33)–(35). This means that the singularities do not result from improper application of the saddle-point technique. From the view point of the calculation procedure, the singularities can disappear only due to taking into account higher-order corrections to the electron functions [Eq. (15)] that are essentially approximate solutions to the time-dependent Schrodinger equation[20] or due to the specific choice of the band structure.[19] Thus, the singularities do not result from violation of the assumptions of the mathematical procedure made in the framework of the Keldysh approach.

Absence of any evident violations of the mathematical-model assumptions forces to search for the physical reasons of the singularities. In this connection, we notice that condition (31) implies the effective-band structure [Eq. (22)] [and Eq. (19) also] to be independent of the initial value of quasimomentum p_0, i.e., the band structure becomes flat over the entire Brillouin zone (Fig. 3). Mechanism of the flattening is related to the radiation-driven electron oscillations[20,21,39,41] and the Bragg-type reflections of the oscillating electrons at

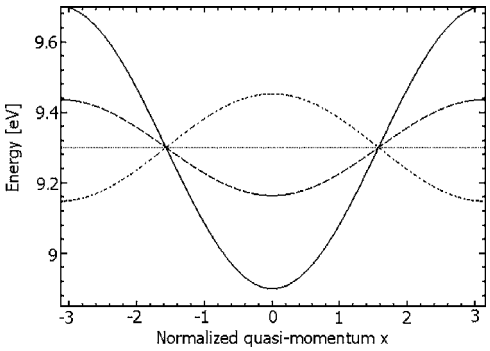

FIG. 3. Variations of the effective-band structure [Eq. (19)] with increasing of laser intensity. Solid curve corresponds to $\chi=0.0$ (initial band), dash curve to $\chi=1.8$, dotted curve to $\chi=\xi_1=2.4048$ (flattening), and dash-dotted curve to $\chi=3.5$ (depicted to show displacement of the initial minimum at the center of the Brillouin zone to the edges at laser intensity $I>I_{th}$).

the edges of the first Brillouin zone. According to the recent interpretation[20,21,39] of the Keldysh model of laser ionization of solids, electron functions [Eq. (15)] imply that each electron oscillates in quasimomentum space under action of electric field of laser radiation and the crystal potential. Correspondingly, the total electron energy described by the effective-band structure [Eq. (14)] has two contributions—the initial energy determined by the band structure of the unperturbed crystal (2) and the pondermotive potential determined by an average energy of the radiation-driven oscillations. It is obvious that electrons occupying initial states near the zone center are effectively accelerated by electric field of the laser radiation[39,45] since their instant energy is larger than their initial energy for most part of the oscillation period (see Fig. 4). This means that the average electron energy increases with laser intensity, and the pondermotive potential is

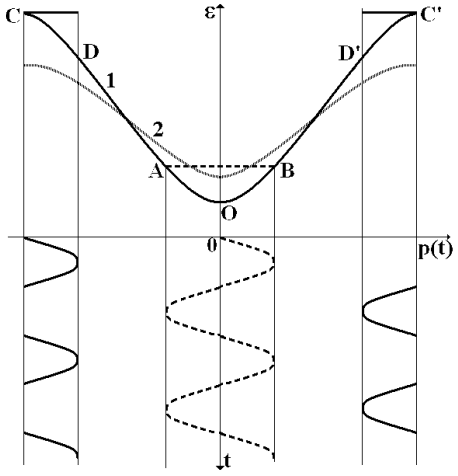

FIG. 4. A sketch of distribution of total energy among the oscillating electrons in BZ. Solid curve in the lower part below lines CD and $C'D'$ depicts oscillations of an electron with initial value of quasimomentum lying exactly on the left edge of the BZ. Dashed curve in the lower part below line AB depicts oscillations of an electron with zero initial quasimomentum. Solid curve 1 depicts the initial band structure; dotted curve 2 depicts the distribution of total energy of the oscillating electrons at nonzero laser intensity.

positive for those electrons. It corresponds to the moving of the central part of the effective-band structure to higher energy with increasing of laser intensity (Figs. 3 and 4).

The electrons occupying initial states near the edges of the first Brillouin zone undergo the radiation-driven oscillations that are perfectly the same as for the above considered center electrons due to the Bragg-type reflections at the edges of the Brillouin zone[39,45] (Fig. 4). In contrary to the electrons occupying initial states near the zone center, the edge electrons are effectively slowed down by the radiation since their initial energy is larger than their instant energy for most part of the oscillation period. Thus, their pondermotive potential is negative, and their total energy decreases with increasing of laser intensity. We thus conclude that for intensity approaching the singularity threshold, laser radiation induces redistribution of the pondermotive potential among the electrons performing radiation-driven oscillations. Simple analysis of expression (19) shows perfect total-energy balance between all the oscillating electrons: the center electrons corresponding to small values of x, y, and z obtain exactly the same amount of the pondermotive energy that is taken away from the edge electrons corresponding to x and y close to $\pm\pi$. As a result, the total energy tends to have constant distribution over the Brillouin zone, and the rigorous flattening of the effective-band structure occurs at $\chi=\xi_K$. Expressions (33)–(35) clearly show that the considered flattening of the effective-band structure is directly related to the singularities.

Substituting Eq. (20) into Eq. (31), one can see that the first flattening corresponding to the first singularity takes place if the amplitude of laser-induced electron oscillations is about 0.76 of half-width of the Brillouin zone. It means that each electron in each energy band passes through most states of the band within one period of its oscillations in this case. Determining an average electron state by averaging over the oscillation period, one can see that the state is the same for all the oscillating electrons of the energy band. Due to that, an averaged probability of an interband jump for each valence electron does not depend on its initial energy and quasimomentum in the Brillouin zone. This leads to two important conclusions related to the flattening: (1) a two-band system degenerates into two-level system, and (2) the value of probability of the interband transition averaged over one period of radiation oscillations is the same for each electron of the valence band (and hole in the conduction band) regardless of its initial state.

Thus, the considered singularities correspond to the specific regime of laser-driven harmonic coherent electron oscillations, resulting in effective energy redistribution and flattening of the effective forbidden band. That leads to intensive and fast excitation of most electrons from the valence band to the conduction band, resulting in the formation of electron-hole plasma with density of an order of 10^{23} 1/cm^3. In any case, laser action induces significant change of the electronic structure of irradiated area of the crystal, inducing further modification of material properties due to the strong perturbation of the initial crystal potential. It means that the material model utilized to describe the photoionization at low laser intensity (i.e., at $0\leqslant\chi<\xi_1$) should be modified as soon as the intensity exceeds the first-singularity threshold I_{th} calculated from Eq. (32). In other words, the first singularity should be considered as a point of possible phase transition. Simple estimations show that for most wide band-gap crystals, the value of I_{th} is about 10 TW/cm^2. The high-order branches of the function [Eq. (27)] corresponding to $I>I_{th}$ must be calculated with a material model modified so as to take into account the modification of the electronic structure. On the other hand, the most critical field-induced variations of the band structure at intensity below the first-singularity threshold [Eq. (32)] are automatically taken into account in our calculations.

According to the presented analysis, the key reason of the singularities is dispersion relation (4) that results in the specific effective-band structure [Eq. (19)]. Effective bands pretty similar to Eq. (19) have also been obtained for other problems[48–52] related to coherent electron effects driven by monochromatic radiation in periodic structures under the approximation of tight binding. For example, we can refer to studies of the coherent effects in one dimensional semiconductor superlattices including collapse of minibands,[48,49] exciton problems,[50] nonlinear optical response,[51] and dynamic electron localization.[52] Moreover, argument of the Bessel functions $J_0(\chi)$ in all those publications[48–52] is given by relation (20) with the upper part of the fraction usually named as the Bloch frequency. Previous analysis of the physical background of the Keldysh model[20,21,39] confirms validity of that name since the Bloch-type oscillations of electrons in the first Brillouin zone are one of the key physical effects of the model. Correspondingly, condition (31) determines threshold of remarkable effects in the tight-binding systems: above considered singularity of the ionization rate in dielectrics, miniband collapse,[48,49] or dynamic electron localization[51,52] in the superlattices. Similarity between the effective-band flattening analyzed above and the collapse of minibands[48,49] leads to the idea that processes similar to the dynamic electron localization can underlie the photoionization suppression at intensity slightly below the first-singularity threshold (Fig. 2).

This line of analogies can be continued from another side. Obviously, the matrix element corresponding to the interband transitions with the effective band [Eq. (19)] must also include the Bessel function $J_0(\chi)$ of the argument Eq. (20) as a factor. Similar structure of matrix elements with the same argument [Eq. (20)] of the Bessel function was obtained for the case of phase transitions in periodic quantum structures driven by monochromatic field,[52,53] e.g., in the Bose-Hubbard periodic system (optical lattice).[53] Correspondingly, it was shown[53] that condition (31) determined the threshold of the phase transition in that system. As we just mentioned above, the same condition [Eq. (31)] determines the threshold of the phase transition in the irradiated dielectric in our problem.

B. Basic assumptions

Deriving the ionization rate [Eq. (27) and (28)] and giving the physical interpretation of the flattening and the singularities, we basically followed the formulation and the main assumptions of the Keldysh model for nonmetallic solids.[19]

The mathematical assumptions have been discussed in Sec. II, and here we concentrate on the assumptions of the physical model.

(1) All collisions of the electrons with each other and with other particles resulting in chaotic variations of electron quasimomentum are neglected.

(2) All perturbations of the band structure and material parameters induced by the photoionization and electric field of the laser radiation are negligibly small.

(3) The photoionization rate is small enough.[20,21]

(4) Contributions of excitons are neglected.

(5) All kinds of many-body effects determining material response to laser action (e.g., polarization and linear and nonlinear optical responses) are neglected.

(6) The radiation is considered to be monochromatic.

Our aim is to analyze which of them are critical for the presented results. First, we consider ideal coherent electron oscillations that are not perturbed by any collisions. That is quite reasonable if one period of the electron oscillations is much smaller than the characteristic time of the collisions resulting in momentum transfer. For laser wavelength of 800 nm, for example, one period of the electron oscillations is 2.5 fs. In the case of shorter wavelengths, the period is even smaller, closer to 1.25 fs for blue visible radiation. Estimations of Bloembergen[54] based on measurements of photoelectron mobility in alkali halides suggest that those values of the oscillation period are slightly less than the characteristic time τ_c of electron-particle collisions with momentum transfer. Recent estimations[13,55] show that for most wide band-gap materials, the momentum-transfer collision time can be much larger than the oscillation period. This gives a serious reason to expect the singularity to take place in real situations in spite of the perturbing influence of the collisions. In that case, the collisions can only decrease the number of the electrons making the interband jumps by factor of $(1-T/\tau_c)$ due to breaking the field-induced synchronization of the electron oscillations.

Second, it is not difficult to show that the first-singularity threshold [Eq. (32)] is well below the electric field F_{cr} induced by ions of the crystal lattice. The latter can be estimated as follows:[21]

$$F_{cr} = \frac{\Delta}{ed}. \tag{36}$$

The ratio of F_{th} to F_{cr} is obtained from Eqs. (32) and (36),

$$\frac{F_{th}}{F_{cr}} = \frac{\hbar\omega}{\Delta}\xi_1. \tag{37}$$

Hence, the singularity threshold F_{th} does not exceed the crystal field F_{cr} if the photon energy is not greater than $\Delta/3$. In the case of $3\hbar\omega \geqslant \Delta$, amplitude of electric field of the laser radiation approaching the singularity threshold produces too much perturbation to the crystal potential which makes the whole Keldysh model invalid for describing the ionization process near the first singularity.

Also, Fig. 2 suggests that the value of the ionization rate is quite small even at intensity close to the singularity threshold. This implies that the perturbations of material parameters induced by the ionization can be neglected at intensity below the singularity point. They become large only if laser intensity is equal or very close to the singularity threshold. This means that specific limitation on the value of the ionization rate characteristic of the Keldysh model[20,21] is not violated except for intensity extremely close to the singularity point. Thus, the perturbations to the material parameters induced by the radiation and the photoionization can be neglected in the first approximation.

Due to the small ionization rate at intensity below the first-singularity threshold, that conclusion is true for the many-body effects determining linear and nonlinear optical responses of ionized material. Therefore, the general self-consistent problem that includes modification of the ionizing field due to the many-body effects can be reduced to the sequence of independent iterations. Correspondingly, the material response can be considered as unperturbed in the first iteration analyzed in this paper, and calculation of electric field ionizing the crystal becomes a separate problem (in general case—nonlinear due to high intensity of radiation) that can be solved after the ionization rate has been calculated in the first approximation. At the next iteration, the distribution of electric field calculated under the influence of the photoionization can be substituted back into the Keldysh procedure to derive small corrections to the first approximation. The situation changes dramatically only at intensity very close or above the first-singularity threshold that can change many-body interactions in the irradiated material so significantly and so fast that the proposed iteration method becomes not valid. In that case, a rigorous self-consistent problem must be analyzed. Thus, one can neglect the many-body effects as high-order contributions to the first approximation at intensity below the first-singularity threshold.

At last, neglecting the exciton contributions can be considered to be rough since production of the excitons accompanies laser ionization of wide band-gap materials.[56–58] It should be noted here that the influence of the excitons becomes pronounced only at low intensity corresponding to low ionization rate since they give a significant contribution to preexponent factor only. At high ionization rate, the density of free electrons in the conduction band is large enough to produce significant screening of the Coulomb-type electron-hole interaction and to prevent exciton generation. Due to that fact, one can neglect the exciton influence on the singularity threshold.

C. Comparison with experimental data

The first singularity should be associated with a certain process observable in experiments. Since it corresponds to the formation of dense electron-hole plasma, a plasma flash produced by laser pulse in bulk of transparent dielectric crystal is a natural candidate to be an experimental manifestation of the singularity. In many cases, the plasma flash is associated with laser-induced breakdown of the dielectric crystals.[3,5,8,11,12] Bearing that in mind, we should examine experimental data on measurements of plasma formation and breakdown thresholds in bulk dielectric crystals and compare them with theoretical predictions obtained from Eq. (32) for

the first-singularity threshold. The predictions include (1) absolute value of the singularity threshold that can be calculated from Eq. (32) and (2) dependence of the threshold on laser frequency and crystal-lattice constant.

First of all, experimental data corresponding to the considered above approximations should be separated out to perform the comparison correctly. The photoionization model under consideration was developed for laser interactions with bulk crystals. It means that the experimental data related to surface interactions (e.g., Refs. 4–6, 9, and 10) cannot be utilized for reliable comparison with the presented theoretical predictions due to the uncontrolled influence of surface states, defects,[54] and impurities that can be critical for reliable measurement of the threshold of plasma formation.

Pulse duration is one of the critical parameters for the reliable comparison with the experiment since it determines which mechanism of the ionization dominates—the photoionization or the avalanche ionization. According to the recent calculations,[13] the photoionization dominates at intensity exceeding a few TW/cm^2 if pulse duration is below approximately 1 ps. Thus, the presented theoretical results should be compared with experimental measurements of plasma-formation and breakdown thresholds by femtosecond laser pulses in bulk wide band-gap dielectric crystals.

The plasma formation has been observed in many experiments performed under the conditions close to those discussed above.[3,8,11,12] One of the main problems is that absolute value of the plasma-formation threshold intensity is extremely difficult to be measured directly.[8,11,12] Due to that problem, the threshold energy of laser pulse is frequently the only available measured characteristic of that process, and the corresponding laser intensity is estimated from various calculation approaches and indirect measurement procedures utilized to extract the threshold intensity.[8,11] Reliability of thus obtained data relies on correctly taking into account the influence of self-focusing, aberrations and other distortions to the focusing that are difficult to account for due to their nonlinear character. Those data provide order of magnitude for the threshold intensity rather than its rigorous value. Bearing that in mind, we find good agreement between the threshold of the first singularity [Eq. (32)] (about 10 TW/cm^2) and the results of measurements (9.8 TW/cm^2 in Ref. 11 and from 16 to 43 TW/cm^2 in Ref. 8 at a wavelength of 800 nm). The problem is that most materials from Refs. 8 and 11 for which the measurements were performed are noncrystalline ones (glasses).

A more reliable way to compare our predictions with the experimental data is to check dependence of the plasma-formation and breakdown thresholds on laser and material parameters. In Ref. 12, a scaling of the damage threshold was reported of the form

$$I_{th}d^2 = \text{const} \tag{38}$$

for several rare-earth fluoride crystals, where I_{th} is the threshold intensity of the plasma formation associated with the laser-induced breakdown, and d is an average inter-ionic distance. That dependence perfectly corresponds to that provided by the threshold [Eq. (32)] with the constant depending on laser wavelength as λ^{-2}. Thus, we have found good quantitative agreement between the experimental data[8,11,12] and the presented theoretical model.

D. Asymptotic limits

Two asymptotic limits are of importance for the analysis of the properties of expressions (27) and (28). The first one corresponds to $\chi \ll 1$ and is essentially the multiphoton limit. It can be obtained by expanding Eq. (27) and (28) into series with respect to the modified adiabatic parameter. By keeping only the zero-order term in the slow amplitude [Eq. (28)] and all terms of the order not exceeding 2 in the exponent, one obtains the following multiphoton-ionization rate:

$$w_{COS}^{MP} = 2\frac{2\omega}{9\pi}\sqrt{\frac{\omega^3}{\hbar\Delta}}\frac{m}{d}\sqrt{u_0\sqrt{\frac{u_c-1}{u_c+1}}}\exp\left[2\frac{\Delta}{u_0\hbar\omega}\sqrt{\frac{u_c+1}{u_c-1}} + \chi^2\frac{\sqrt{u_c^2-1}}{u_0^3}\left(\frac{\Delta}{\hbar\omega}-\alpha\right)\right]\exp\left\{\left(\frac{\Delta}{\hbar\omega}\frac{u_c}{u_c-1}-\alpha\right) \times\left(1+\frac{\chi^2}{4}\right)\left[\frac{u_0^2}{2}\left(1+\frac{u_0^2}{24}\right)-2\frac{\sqrt{u_c^2-1}}{u_0}+\frac{u_0^6}{2160}\right]\right\} \times\left(\frac{\chi^2}{4u_0^2}\right)^{\alpha}\Phi(\beta), \tag{39}$$

where

$$\alpha = \left\langle \frac{E_{MP}}{\hbar\omega}+1 \right\rangle \tag{40}$$

is the number of the absorbed photons, and the argument of the Dawson integral is

$$\beta = \sqrt{2\frac{\sqrt{u_c^2-1}}{u_0}\left(\alpha-\frac{E_{MP}}{\hbar\omega}\right)\left(1+\chi^2\frac{u_0^2-2}{4u_0^2}\right)}, \tag{41}$$

with effective band gap in the multiphoton limit given by

$$E_{MP} = \Delta\left[1+\frac{\chi^2}{4(u_c-1)}\right]. \tag{42}$$

The opposite limit corresponds to the singularity and can be derived under the condition $\chi \to \xi_1$. Keeping only the terms of the lowest order, one gets the following singularity asymptotic:

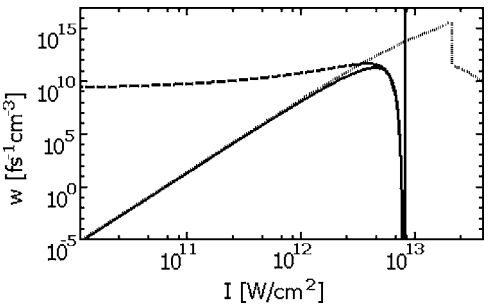

FIG. 5. Dependence of the ionization rate w given by Eq. (27) (solid curve) on laser intensity I together with the multiphoton (dotted curve) and singularity (dash curve) asymptotic limits given by expressions (39) and (43) correspondingly. Laser wavelength is 830 nm; material parameters correspond to NaCl.

$$w_{COS}^{S} = 2\frac{2\omega}{9\pi}\sqrt{\frac{\omega^3}{\hbar\Delta}}\frac{m}{d}\exp\left\{\frac{1}{J_1(\xi_1)\delta}\left(\alpha_S - \frac{u_c}{u_c-1}\frac{\Delta}{\hbar\omega}\right)\left[\sqrt{\frac{u_c^2-1}{\theta}} - u_0 f_1(\xi_1)\right]\left[2 - \frac{\delta}{\xi_1} + \frac{\delta(2\xi_1^2-1)}{6\xi_1^2}\right]\right\}$$
$$\times\exp\left\{\frac{\Delta}{\hbar\omega}\frac{2}{u_c-1}\left[\sqrt{\frac{u_c^2-1}{\theta}} - u_c\sinh^{-1}\left(\frac{u_0}{\xi_1}\right) + \frac{\delta}{\sqrt{\theta}}\left(\frac{\xi_1\sqrt{u_c^2-1}}{\theta} - \frac{u_0 u_c}{\xi_1}\right)\right]\right\}\sqrt{\frac{\theta}{8J_1(\xi_1)\delta(u_c+1)\left(\alpha_S - \frac{E_S}{\hbar\omega}\right)}}$$
$$\times\exp\left\{\frac{1}{J_1(\xi_1)}\left(\alpha_S - \frac{u_c}{u_c-1}\frac{\Delta}{\hbar\omega}\right)\left[\left(u_0 f_{11} + \xi_1\frac{\sqrt{u_c^2-1}}{\theta^{1.5}}\right)\left(2 - \frac{\delta}{\xi_1}\right) - \delta\left(u_0 f_{12} - \sqrt{\frac{u_c^2-1}{\theta}}\frac{2\xi_1^2 - u_0^2}{\theta^2}\right)\right]\right\}, \quad (43)$$

where

$$\alpha_S = \left\langle \frac{E_S}{\hbar\omega} + 1 \right\rangle \quad (44)$$

is again the number of the absorbed photons, and several notations are introduced to shorten expression (43),

$$\delta = \xi_1 - \chi, \quad (45)$$

$$\theta = \xi_1^2 + u_0^2, \quad (46)$$

$$E_S = \Delta\left[\frac{u_c}{u_c-1} - \frac{J_1(\xi_1)}{u_c-1}\delta\right], \quad (47)$$

$$f_{11} = -\xi_1\int_0^1 \frac{\cosh(u_0 s)}{(\xi_1^2 + u_0^2 s^2)^{1.5}}ds,$$

$$f_{12} = \frac{f_{11}}{\xi_1} + 3\xi_1^2\int_0^1 \frac{\cosh(u_0 s)}{(\xi_1^2 + u_0^2 s^2)^{2.5}}ds. \quad (48)$$

Here, $J_1(x)$ is the Bessel function of the first kind and the first order.

Plotting the asymptotic expressions together with the rate [Eq. (27)] (Fig. 5), one can see two characteristic features. First, the multiphoton asymptotic [Eq. (39)] coincides with the complete rate [Eq. (27)] practically up to the singularity threshold. This means that the photoionization stays in the multiphoton regime until the singularity, and no tunneling can be observed for the lowest-order branch of the ionization rate. Second, analysis of the first exponent in Eq. (43) allows us to explain the specific behavior of the ionization rate in the vicinity of the singularity point (Fig. 2) since the exponent determines a dominating contribution to the asymptotic. The factor of the exponent,

$$a_1 = \sqrt{\frac{u_c^2-1}{\theta}} - u_0 f_1(\xi_1), \quad (49)$$

is negative for all values of laser and material parameters. Thus, increasing or decreasing of the ionization rate near the singularity point is determined by the other factor,

$$a_2 = \alpha_S - \frac{u_c}{u_c-1}\frac{\Delta}{\hbar\omega}. \quad (50)$$

The sign of a_2 is not constant; it can vary from positive to negative in certain cases. In the case of negative values of a_2, the exponent grows up to infinity monotonously without dropping to zero. Equation (50) gives the following condition for the photon energy to obtain the monotonous increasing of the ionization rate near the first-singularity point:

$$\hbar\omega \leqslant \frac{\Delta u_c}{\alpha_S(u_c-1)}, \quad (51)$$

where the number of absorbed photons α_S is an integer according to Eq. (44). Equation (51) gives the upper limit of the photon energy, while the lowest limit is determined by the obvious condition

$$\hbar\omega \geqslant \frac{E_S}{\alpha_S}. \quad (52)$$

Comparing Eqs. (51) and (52) with the account of Eq. (47), one comes to conclusion that the monotonous increasing of the ionization rate near the singularity point is possible only for the monochromatic radiation of the following frequency:

$$\omega = \frac{\Delta u_c}{\hbar\alpha_S(u_c-1)}. \quad (53)$$

The opposite relation $a_2 > 0$ makes the exponent decrease and, thus, causes photoionization suppression (Fig. 2), i.e., ionization rate decreases to zero when approaching the singularity point. The condition for the photon energy providing this regime is as follows:

$$\hbar\omega \geqslant \frac{\Delta u_c}{\alpha_S(u_c-1)}. \quad (54)$$

It is met by all laser frequencies except those given by Eq. (53). Thus, we conclude that specific ionization suppression is possible in the vicinity of the singularity point, depending on laser wavelength and material parameters.

IV. CONCLUSIONS

Utilizing the Keldysh approach,[19] we have analytically calculated the photoionization rate for cosine energy-

momentum relation (4) characteristic of the approximation of tight binding. That approximation is specific of wide band-gap materials. Its special feature is the zero slopes at the edges of the first Brillouin zone that allows correctly describing the Bragg-type reflections of coherently oscillating electrons at the edges of the zone. Being combined with the radiation-driven electron oscillations, the reflections result in specific ionization effects (singularities on the dependence of the ionization rate on laser and material parameters, ionization suppression near the singularity points, and the flattening of the effective-band structure) not provided by energy-momentum relations (3) and (10) traditionally utilized in ionization-rate calculations.[18–35] Due to the reflections, the ionization rate becomes a multibranch function of laser and material parameters with different branches separated by the singularity points. We have shown that the Keldysh approximation corresponds to the lowest-order branch of the function that lies completely in the multiphoton regime except a small vicinity of the first-singularity point.

Investigating the singularity points, we have shown that a two-band quantum system degenerates into two-level system at each singularity point since the effective-band structure becomes flat over the entire Brillouin zone at laser intensity corresponding to the singularities. As a result of the flattening, all valence-band electrons have the same value of interband transition probability at those values of laser intensity. That results in extremely high values of the ionization rate at the singularity points.

The key points of the physical model underlying the cosine-band model [Eq. (4)] and the presented above calculations are (1) space periodicity, (2) approximation of tight binding, (3) dominating contribution of the nearest-neighbor interactions in the formation of the crystal potential, and (4) coherent electron oscillations driven by monochromatic radiation. They are characteristic of other periodic systems, e.g., semiconductor superlattices[48–52] and Bose-Hubbard periodic optical lattice[58] driven by external harmonic radiation and provide remarkable cross connections between the effects discussed in this paper and the specific effects in those systems. Summarizing those cross connections, we come to a conclusion that the above presented specific effects (flattening of the effective band structure, the related singularities, and expected phase transitions at the singularity point) are characteristic of coherent electron oscillations driven by harmonic external field in a periodic quantum system described in the framework of tight-binding approximation with strong nearest-neighbor interactions.

All those effects demonstrate a very strong qualitative influence of the functional form of the energy-momentum relation on the process of photoionization and the value of its rate at high laser intensities. In the considered case of the dielectric crystals, the influence becomes significant at intensity exceeding approximately 1 TW/cm^2.

We have also demonstrated that the definition of the adiabatic parameter is completely determined by the energy-momentum relation. In particular, the traditional definition [Eq. (1)] corresponds to the Kane-type band structure [Eq. (10)], while cosine relation (4) results in different form [Eq. (20)] of the parameter. In particular, the adiabatic parameter [Eq. (20)] does not depend on the effective electron (or reduced effective electron-hole) mass since the band structure [Eq. (4)] allows going beyond the approximation of constant effective electron mass. Thus, the considered effects should also be attributed to the specific dependence of the effective mass on electron quasimomentum that is usually dropped in theoretical calculations including the most recent improvements of the Keldysh model.[29–35]

We have shown that the Keldysh approach does not allow evaluation of the ionization rate at the singularity points and beyond the first singularity, but it provides a rigorous expression for the threshold of the first singularity. Obtained values of the threshold [Eq. (32)] have been found to be in good agreement with data of experimental measurements[8,11,12] of the threshold intensity for production of plasma flash in transparent solids.

ACKNOWLEDGMENTS

The author wishes to thank Academicians of Russian Academy of Sciences L. V. Keldysh (Physics Institute of RAS) and N. B. Delone (General Physics Institute of RAS), M. V. Fedorov, S. V. Garnov, and V. P. Krainov (General Physics Institute of RAS), and V. L. Komolov and S. G. Przhibel'sky (S. I. Vavilov State Optical Institute) for their questions, comments and discussions of results put into the basics of this paper.

[1] A. M. Bonch-Bruevich and V. A. Khodovoy, Sov. Phys. Usp. **85**, 3 (1965).
[2] V. Nathan, A. H. Guenther, and S. S. Mitra, J. Opt. Soc. Am. B **2**, 294 (1985).
[3] D. von der Linde and H. Schüller, J. Opt. Soc. Am. B **13**, 216 (1996).
[4] M. Lenzner, J. Kruger, S. Sartania, Z. Cheng, C. Spielmann, G. Mourou, W. Kautek, and F. Krausz, Phys. Rev. Lett. **80**, 4076 (1998).
[5] A. C. Tien, S. Backus, H. Kapteyn, M. Murnane, and G. Mourou, Phys. Rev. Lett. **82**, 3883 (1999).
[6] M. Li, S. Menon, J. P. Nibarger, and G. N. Gibson, Phys. Rev. Lett. **82**, 2394 (1999).
[7] R. Stoian, D. Ashkenasi, A. Rosenfeld, and E. E. B. Campbell, Phys. Rev. B **62**, 13167 (2000).
[8] C. Schaffer, A. Brodeur, and E. Mazur, Meas. Sci. Technol. **12**, 1784 (2001).
[9] I. H. Chowdhury, A. Q. Wu, X. Xu, and A. M. Weiner, Appl. Phys. A: Mater. Sci. Process. **81**, 1627 (2005).
[10] A. Q. Wu, I. H. Chowdhury, and X. Xu, Phys. Rev. B **72**, 085128 (2005).
[11] O. Efimov, S. Juodkazis, and H. Misawa, Phys. Rev. A **69**, 042903 (2004).
[12] S. Juodkazis, T. Kondo, A. Rode, E. Gamaly, S. Matsuo, and H.

Misawa, Proc. SPIE **5662**, 179 (2004).
[13] B. Rethfeld, Phys. Rev. B **73**, 035101 (2006).
[14] R. Braunstein, Phys. Rev. **125**, 475 (1962).
[15] R. Braunstein and N. Ockman, Phys. Rev. **134**, A499 (1964).
[16] J. H. Yee, Phys. Rev. B **3**, 355 (1971).
[17] J. H. Yee, Phys. Rev. B **5**, 449 (1972).
[18] A. Vaidyanathan, A. H. Guenther, and S. S. Mitra, Phys. Rev. B **24**, 2259 (1981).
[19] L. V. Keldysh, Sov. Phys. JETP **20**, 1307 (1965).
[20] V. E. Gruzdev, J. Phys.: Condens. Matter (to be published).
[21] V. E. Gruzdev, J. Opt. Technol. **71**, 14 (2004).
[22] H. D. Jones and H. R. Reiss, Phys. Rev. B **16**, 2466 (1977).
[23] M. H. Weiler, Phys. Rev. B **7**, 5403 (1973).
[24] F. Adduci, I. M. Catalano, A. Cingolani, and A. Minafra, Phys. Rev. B **15**, 926 (1977).
[25] Y. A. Bychkov and A. M. Dykhne, Sov. Phys. JETP **31**, 928 (1970).
[26] F. M. H. Faisal, J. Phys. B **6**, L89 (1973).
[27] H. R. Reiss, Phys. Rev. A **22**, 1786 (1980).
[28] H. S. Brandi, L. Davidovich, and N. Zagury, Phys. Rev. A **24**, 2044 (1981).
[29] A. Vaidyanathan, T. W. Walker, A. H. Guenther, S. S. Mitra, and L. M. Narducci, Phys. Rev. B **20**, 3526 (1979).
[30] H. R. Reiss, Phys. Rev. A **42**, 1476 (1990).
[31] P. W. Milonni, Phys. Rev. A **45**, 2138 (1992).
[32] H. R. Reiss, Phys. Rev. A **45**, 2140 (1992).
[33] D. Bauer, D. B. Milosevic, and W. Becker, Phys. Rev. A **72**, 023415 (2005).
[34] G. F. Gribakin and M. Yu. Kuchiev, Phys. Rev. A **55**, 3760 (1997).
[35] K. Mishima, M. Hayashi, J. Yi, S. H. Lin, H. L. Selzle, and E. W. Schlag, Phys. Rev. A **66**, 033401 (2002).
[36] S. D. Chao, Phys. Rev. A **72**, 053414 (2005).
[37] A. Kovarskii and E. Y. Perlin, Phys. Status Solidi B **45**, 47 (1971).
[38] E. O. Kane, J. Phys. Chem. Solids **1**, 249 (1957).
[39] V. E. Gruzdev, in *Laser Ablation*, edited by C. H. Phipps (Springer, New York, 2006), pp. 99–121.
[40] V. L. Bonch-Bruevich and S. G. Kalaschnikov, *Halbleiterphysik* (VEB, Berlin, 1982), Chaps. 3 and 4.
[41] L. V. Keldysh, Sov. Phys. JETP **6**, 763 (1958).
[42] J. Callaway, *Energy Band Theory* (Academic, New York, 1964).
[43] R. T. Poole, J. G. Jenkin, J. G. Liesegang, and R. C. Leckey, Phys. Rev. B **11**, 5179 (1975).
[44] D. B. Sirdeshmikh, L. Sirdeshmukh, and K. G. Subhadra, *Alkali Halides: A Handbook of Physical Properties* (Springer-Verlag, Berlin, 2001).
[45] V. E. Gruzdev, J. Opt. Technol. **73**, 385 (2006).
[46] A. Vaidyanathan, T. Walker, A. H. Guenther, S. S. Mitra, and L. M. Narducci, Phys. Rev. B **21**, 743 (1980).
[47] M. V. Fedoryuk, *Saddle-Point Method* (Nauka, Moscow, 1977), Chap. IV.
[48] M. Holthaus, Phys. Rev. Lett. **69**, 351 (1992).
[49] M. Holthaus and D. Hone, Phys. Rev. B **47**, 6499 (1993).
[50] P. Ray and P. K. Basu, Phys. Rev. B **50**, 14595 (1994).
[51] T. Meier, G. von Plessen, P. Thomas, and S. W. Koch, Phys. Rev. B **51**, 14490 (1995).
[52] D. H. Dunlap and V. M. Kenkre, Phys. Rev. B **34**, 3625 (1986).
[53] A. Eckardt, C. Weiss, and M. Holthaus, Phys. Rev. Lett. **95**, 260404 (2005).
[54] N. Bloembergen, IEEE J. Quantum Electron. **QE-10**, 375 (1974).
[55] E. G. Gamaly, O. P. Uteza, A. V. Rode, M. J. Samoc, and B. Luther-Davies, Proc. SPIE **6261**, 283 (2006).
[56] P. Audebert, Ph. Daguzan, A. Dos Santos, J. C. Gauthier, J. P. Geindre, S. Guizard, G. Hamoniaux, K. Krastev, P. Martin, G. Petite, and A. Antonetti, Phys. Rev. Lett. **73**, 1990 (1994).
[57] S. Guizard, P. Martin, G. Petite, P. D'Oliveira, and P. Meynadier, J. Phys.: Condens. Matter **8**, 1281 (1996).
[58] F. Quere, S. Guizard, and Ph. Martin, Europhys. Lett. **56**, 138 (2001).